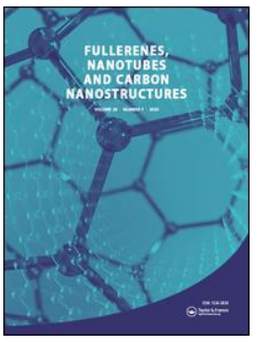

Taylor & Francis
Taylor & Francis Group

Fullerenes, Nanotubes and Carbon Nanostructures

ISSN: (Print) (Online) Journal homepage: https://www.tandfonline.com/loi/lfnn20

# Radical character of non-IPR isomer 17418 ($C_1$) of fullerene $C_{76}$

Ayrat Khamatgalimov, Anna Egorova, Denis Chachkov & Valeri Kovalenko

**To cite this article:** Ayrat Khamatgalimov, Anna Egorova, Denis Chachkov & Valeri Kovalenko (2021): Radical character of non-IPR isomer 17418 ($C_1$) of fullerene $C_{76}$, Fullerenes, Nanotubes and Carbon Nanostructures, DOI: 10.1080/1536383X.2021.1880393

**To link to this article:** https://doi.org/10.1080/1536383X.2021.1880393

View supplementary material

Published online: 03 Feb 2021.

Submit your article to this journal

Article views: 36

View related articles

View Crossmark data

Full Terms & Conditions of access and use can be found at
https://www.tandfonline.com/action/journalInformation?journalCode=lfnn20

FULLERENES, NANOTUBES AND CARBON NANOSTRUCTURES
https://doi.org/10.1080/1536383X.2021.1880393

Taylor & Francis
Taylor & Francis Group

Check for updates

# Radical character of non-IPR isomer 17418 ($C_1$) of fullerene $C_{76}$

Ayrat Khamatgalimov[a], Anna Egorova[b], Denis Chachkov[c], and Valeri Kovalenko[a]

[a]Arbuzov Institute of Organic and Physical Chemistry, FRC Kazan Scientific Center, Russian Academy of Sciences, Kazan, Russia; [b]Kazan National Research Technological University, Kazan, Russia; [c]Kazan Department of Joint Supercomputer Center of Russian Academy of Sciences, FSC Scientific Research Institute for System Analysis, Russian Academy of Sciences, Kazan, Russia

**ABSTRACT**

Using a theoretical approach supported by DFT calculations, the features of molecular structure of isomer 17418 ($C_1$) of fullerene $C_{76}$ with the distribution of single, double and delocalized $\pi$-bonds has been determined for the first time. It is shown the radical nature together with the well-known overstrain due to pentalene fragment are the reasons for the instability of this fullerene as empty molecule. The synthesis of endohedral metallofulerenes is accompanied by the formation of an ion pair: the fullerene anion and a metal cation inside the molecule. It's leading to the closure of the electron shell of the fullerene molecule and the removal of excess local strains. The previously experimentally determined cations sites inside the fullerene, which stabilize the molecule as a whole, are close to the disclosed radical clusters.

**ARTICLE HISTORY**
Received 12 January 2021
Accepted 20 January 2021

**KEYWORDS**
Fullerene $C_{76}$; structural formula; substructure; radical; overstrain

## 1. Introduction

Nearly 100 of higher fullerenes that do not obey the Isolated Pentagon Rule (IPR)[1,2] have been produced last two decades as endohedral or exohedral derivatives.[3] All of them are synthesized by chance i.e., at the start no one has known what would appear on the finish. One of the reasons for such uncertainty is very limited knowledge of the molecular structure of pristine non-IPR fullerene. All non-IPR fullerenes are well-known to be unstable as pristine ones. However, fullerene cages including non-IPR ones are often become stable as exohedral or endohedral derivatives.

The concept of substructures developed by us has shown its usefulness in studying the stability of higher IPR fullerenes.[4–6] Briefly, by a substructure we call a fragment of a fullerene molecule which is connected with the rest of its part by single bonds, the latter poorly transmit the electron density due to the curvature of the fullerene shell. Therefore, the substructure retains its features regardless of which fullerene molecule it belongs to. Due to this, we have shown that higher IPR fullerenes have substructures characteristic for stable molecules (Figure 1a–c), as well as there are substructures with radical nature (Figure 1e,f) inherent for unstable fullerenes.[4–6]

It is easy to see that perylene substructure can be represented as neutral (Figure 1d) or as two fused phenalenyl-radical substructures (Figure 1f) with a common hexagon (Figure 1e). According to structural data (mainly, single crystal X-ray diffraction analysis), a significant part of IPR fullerenes were obtained only as derivatives: endohedral or exohedral (see, for example,[7–9]). It turned out that they all contain either phenalenyl-radical or perylene substructures that indicate the radical nature of these molecules, i.e., their instability or impossibility of obtaining as pristine fullerenes. For the non-IPR fullerenes, it is often considered that adjacent pentagons in their molecules are the reason for their instability.

$C_{76}$ fullerene has 19151 classical cage isomers, among which two isomers 19150 ($D_2$) and 19151 ($T_d$) satisfy the IPR.[10] Only one IPR isomer 19150 ($D_2$) has been successfully isolated and characterized by single crystal X-ray,[11,12] the second one 19151 ($T_d$) has never been produced due to its unstable open-shell electronic structure.[13,14] A detailed topological study regarding the $C_{76}$ isomers has been done; the definition of a method for calculating the features, number of lines and relative intensities, of the $^{13}C$ NMR theoretical spectrum is presented.[15] Although a set of molecules with touching pentagons that are able to fit the experimental resonance data has been discovered,[15] no experimental evidence has been founded yet for the existence of such molecules as pristine fullerenes. A series of quantum-chemical calculations confirmed that the experimentally obtained isomer 19150 ($D_2$) of $C_{76}$ fullerene to be most energetically favorable.[16–21] Nevertheless, both isomers were produced as various derivatives (endohedral and exoherdal ones). For the stable isomer 19150 ($D_2$) there are several such examples (for example, Yb@$C_{76}$,[22] Sm@$C_{76}$,[23] $C_{76}(CF_3)_{6,8,10,12,14,16,18}$[24–27]), while for 19151 ($T_d$) isomer there is a limited number of such derivatives: the first $T_d$-symmetric metallofullerene has been synthesized, isolated and characterized as $Lu_2$@$C_{76}$,[28] the first experimental

CONTACT Ayrat Khamatgalimov ayrat_kh@iopc.ru Arbuzov Institute of Organic and Physical Chemistry, FRC Kazan Scientific Center, Russian Academy of Sciences, 8 Arbuzova Str., Kazan 420088, Russia.

Supplemental data for this article can be accessed at https://doi.org/10.1080/1536383X.2021.1880393.

© 2021 Taylor & Francis Group, LLC

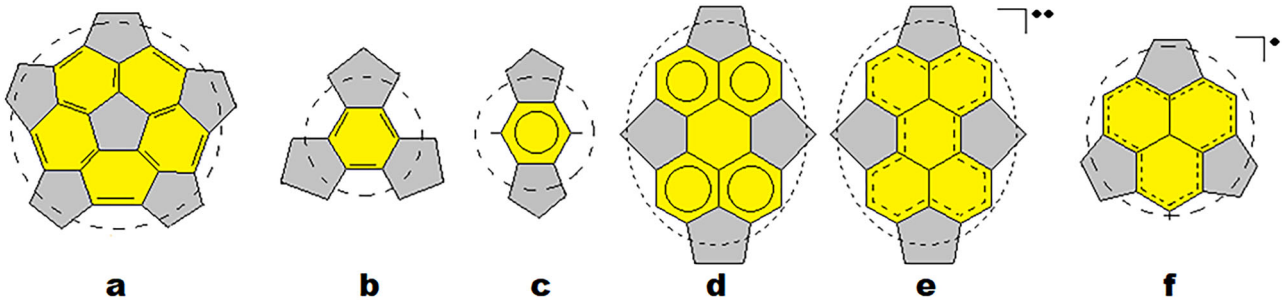


**Figure 1.** Characteristic substructures of fullerene molecules: corannulene (a), sumanene (b), s-indacene (c), perylene (d and e), phenalenyl-radical (f).

evidence for the existence of the hollow $C_{76}$ ($T_d$) fullerenes was represented as exohedral $C_{76}(CF_3)_{12}$.[9]

Additionally to IPR-satisfying, derivatives of fullerene $C_{76}$ were also successfully synthesized and isolated in the form of various non-IPR $C_{76}$ cages. Stabilization of such strained non-IPR fullerene cage due to fused pentagons can be fulfilled by either endohedral or exohedral derivatization. So, the first non-IPR $C_{76}$ cage was synthesized in the form of endohedral metallofullerene $DySc_2N@C_{76}$ as isomer 17490 ($C_s$) having two pairs of the adjacent pentagons.[29] This isomer has been isolated also as $La_2@C_{76}$ and its structure determined from X-ray crystallographic analysis.[30] The theoretical research shows that in the relevant temperature region, the $La_2@C_{76}$ should be considerably more populated compared to $La@C_{76}$ with IPR $T_d$-cage.[31]

Another two non-IPR isomers 19138 ($C_{2v}$) and 17459 ($C_1$) with one pair of adjacent pentagons are obtained experimentally as $Yb@C_{76}$ and investigated by density functional characterization.[32] Later, isomer 19138 ($C_{2v}$) was also produced as $Sm@C_{76}$,[33] $TbNC@C_{76}$ and $YNC@C_{76}$[34] and characterized by single-crystal X-ray diffraction; a combined study of single-crystal X-ray diffraction and DFT calculations suggests that the endohedral $Sm^{2+}$ ion is close to the fused pentagon unit.[33] DFT calculations shows that this isomer is nearly isoenergetic with 17459 ($C_1$) for $M@C_{76}$ (M = Sm,[32,35] Ca, Sr, Ba,[32,36] ScCN and YCN,[37,38] and $Sc_2S$[39]). The recent report on actinide metallofullerenes $U@C_{76}$ presented a successfully synthesized and fully characterized (incl. single crystal X-ray diffractometry) as another non-IPR cage 17418 ($C_1$)[40] that previously was theoretically studied for Th@C76.[41]

Concerning exohedral derivatives of non-IPR isomers, 18917 ($C_2$) cage having five pairs of fused pentagons was produced as $C_{76}Cl_{24}$; it is a first case of non-degradative skeletal rearrangement in fullerenes: a stable IPR $D_2$-$C_{76}$ fullerene underwent a deep transformation of its cage.[42,43] The simultaneous with isomer 18917 ($C_2$) formation of isomer 18387 ($C_1$) is observed for exohedral $C_{76}Cl_{30}$.[44,45] High-temperature chlorination of an IPR $D_2$-$C_{76}$ fullerene followed by high-temperature trifluoromethylation of non-IPR $C_{76}$ chlorides with $CF_3I$ unexpectedly resulted in a series of non-IPR $C_{76}(CF_3)_nF_m$ compounds.[46] X-ray diffraction study with the use of synchrotron radiation revealed the isomer 18917 ($C_2$) with mixed $CF_3$/F structures of non-IPR $C_{76}(CF_3)_{14}$, $C_{76}(CF_3)_{14}F_2$, and $C_{76}(CF_3)_{16}F_6$.[46]

Thus, to date, there are several non-IPR isomers of fullerene $C_{76}$ that are stabilized in the form of various derivatives. Our notion concerning molecular structures and stability of higher IPR fullerenes have shown the usefulness and anticipation of the concept of substructures.[4–6] Here we investigated the molecular structure of lowest symmetry molecule of non-IPR fullerene $C_{76}$ that molecular topology was recently revealed by single-crystal X-ray diffraction of endohedral $U@C_{76}$ as isomer 17418 ($C_1$)[40] according to the early developed approach[4–6] to establish its structure and reasons for stabilizations.

## 2. Methodology and computational details

Previously, we showed that the fullerene molecule could be considered as a set of substructures.[4–6] We developed an approach that provides a complete structural formula of fullerene with the distribution of single bonds, double bonds and $\pi$-delocalized bonds prior to the quantum-chemical calculations. In fact, the analysis of all IPR and some non-IPR molecular structures of higher fullerenes, such as $C_{66}$, $C_{68}$, $C_{72}$, $C_{74}$, $C_{76}$, $C_{78}$, $C_{80}$, $C_{82}$, $C_{84}$, and $C_{86}$, and some isomers of small fullerenes $C_{40}$ and $C_{50}$, confirmed this substructure concept (see Refs. [4–6, 47–49] and references herein).

The preliminary obtained results of the geometrical and electronic structures were verified by quantum-chemical DFT calculations. All calculations were accomplished using the Gaussian'09 program packages.[50] The molecular structures of the researched structures were fully optimized using DFT B3LYP functional[51,52] with 6-31G basis set. The geometry optimizations were performed without the symmetry constraints considering the low symmetry of the studied molecules. The standard keywords, default cutoffs on forces and step size at structural optimizations were used. To improve energies, geometry optimization was followed by single-point calculations with 6-31G(d) and 6-31 + G(d) basis sets. The calculations have shown a good agreement between the results obtained for all used basis sets.

Because the researched structures were suggested also as molecules with the open-shell electronic structures, the quantum-chemical calculations were carried out also in configurations with high multiplicities using the unrestricted Kohn – Sham methodology. To ensure the calculated structures were indeed minima, vibrational analyses were performed using the same methods. The tests of the stability of wave functions were carried out.

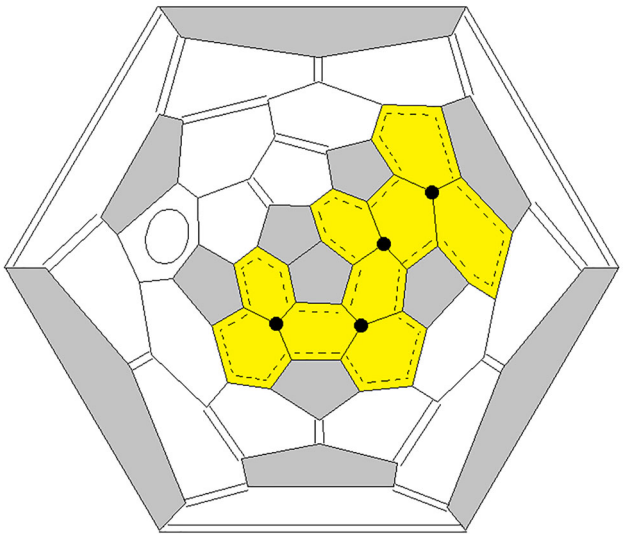

**Figure 2.** Schlegel diagram of non-IPR isomer 17418 ($C_1$) of fullerene $C_{76}$ with open-shell electronic shell. Single and double bonds are depicted by one and two lines, delocalized $\pi$-bonds are designated by a circle or dashed lines; all pentagons are in gray; the proposed radical cluster is highlighted in yellow; bold points indicate the central carbon atoms of four fused phenalenyl-radical substructures.

## 3. Results and discussion

According to our theoretical approach,[4–6] we determined for the first time the distributions of single, double and delocalized $\pi$-bonds (i.e., their molecular formulas) (Figure 2). Analysis of studied fullerene shows the presence of a certain number of corannulene (Figure 1a), sumanene (Figure 1b) and *s*-indacene (Figure 1c) substructures. These substructures are characteristic for the most stable fullerenes $C_{60}$, $C_{70}$ and other produced and characterized IPR fullerenes[4–6] that indicate they cannot be the cause of the instability of the studied molecule.

A cluster consisting of four fused phenalenyl-radical substructures (or two fused perylenes) has a special interest (Figure 2). Interestingly, a similar substructure of two fused perylenes was previously found in the IPR isomer 39714 ($C_2$) of $C_{82}$ fullerene[53] that was obtained and characterized only in the form of various endohedral derivatives.[4,5,54–56] This substructure is clustering with pentalene fragment and represents a new substructure that has not been studied before. First of all, it has recently been shown that the molecules of some pentalene derivatives have an open electron shell with two unpaired electrons.[57] Secondly, the $C_8$ pentalene framework has a planar structure, as well as its derivatives, while in fullerenes the curvature of the fullerene spheroid significantly distorts the planar structure of the pentalene fragment, which was considered to be the cause of the instability of fullerenes with such a fragment.

Thus, the possible radical nature together with the well-known overstrain due to pentalene fragment[6,58,59] can presumably be the reasons of the instability of this fullerene as empty molecule.

Further, to confirm the obtained preliminary conclusions and to choose the true nature of the electronic structure of the isomer under study, quantum-chemical calculations were carried out, including in configurations with high multiplicities. Quantum-chemical calculations show that singlet configuration with closed electron shell and large HOMO-LUMO gap is most energetically favorable (Table 1). Notwithstanding, bearing in mind the above arguments for radical nature of isomer 17418 ($C_1$) of fullerene $C_{76}$, additional analysis of the results of quantum-chemical calculations is required to choose the true nature of its electronic structure. So, DFT calculations were carried out in configurations with high multiplicities using the unrestricted Kohn–Sham methodology: with two and four unpaired electrons (multiplicity is 3 and 5, respectively).

It turned out that the loss of 8 and 32 kcal/mol for multiplicity 3 and 5, respectively, is compensated by a significant gain in the energy of ionic forms. It should be noted that the $C_{76}^{4-}$ and $C_{76}^{6-}$ anions of non-IPR isomer 17418 ($C_1$) becomes more energetically favorable even in comparison with the IPR isomer 19150 ($D_2$) (Table 2).

As a matter of fact, the preliminary bonds distributions according to the developed approach[4–6] are confirmed in DFT calculations: the values of most calculated bond lengths correspond to expected bond types (single, double and delocalized) plotted on Schlegel diagrams and are also in agreement with the well-known experimental values for most stable $C_{60}$ and $C_{70}$ fullerenes[60,61] (Table 3 and supplementary material Table S1). Nevertheless, it should be noted that there are some differences between calculated values and originally proposed bonds distribution according to our theoretical approach.[4–6] Analysis of calculated bonds distribution for various electronic configurations (see Figure S1 in supplementary material) shows that most of the delocalized bonds are arranged in proposed phenalenyl-radical substructures; there are only minor differences between their arrangements for multiplicities 3 and 5. Also, due to lowest symmetry of molecule we cannot use symmetry decrease for estimation number of unpaired electrons. That is why, to determine the exact number of unpaired electrons we are analyzing spin density distributions and compare it with experimentally X-ray determined positions of uranium atoms (cations) inside the molecule.

As expected, the spin densities are mainly concentrated on atoms of fused pentagons and phenalenyl-radical substructures (Figure 3 and supplementary material Table S2). From the analysis of DFT calculation results it was revealed that configuration with two unpaired electrons (triplet) is most preferred. This conclusion is rationalized by the fact that part of the spin densities in quintet configurations is outside of the phenalenyl-radical substructures (depicted by yellow on Figure 3).

The spin densities distribution predetermines a position of a metal atom(s) inside endohedral derivatives. It will be useful for predictions of endohedral atom(s) position inside its endohedral derivatives synthesized in the future or the order of radical addition in reactions of exohedral derivatives synthesis. Earlier we revealed that endohedral metal ions are located close to radical substructures with the most concentrated spin densities.[53] As was mentioned early, the studied non-IPR isomer 17418 ($C_1$) of fullerene $C_{76}$ have been successfully synthesized as actinide endohedral

**Table 1.** Relative energies $\Delta E$ (kcal mol$^{-1}$) and HOMO-LUMO gaps (eV) of non-IPR isomer 17418 ($C_1$) together with most stable IPR isomer 19150 ($D_2$) of fullerene $C_{76}$.

| | $\Delta E$ | | | HOMO-LUMO | | |
|---|---|---|---|---|---|---|
| Isomer no. | 6-31G | 6-31G* | 6-31+G* | 6-31G | 6-31G* | 6-31+G* |
| 19150 ($D_2$) singlet, M = 1[a] | 0.00 | 0.00 | 0.00 | 1.99 | 1.97 | 1.95 |
| 17418 ($C_1$) singlet, M = 1 | 33.10 | 33.75 | 31.23 | 1.30 | 1.30 | 1.28 |
| triplet, | 40.74 | 41.51 | 39.02 | 0.62 | 0.63 | 0.62 |
| M = 3 | 66.36 | 66.00 | 63.40 | 0.14 | 0.09 | 0.11 |
| quintet, M = 5 | | | | | | |

[a]Most stable IPR isomer of fullerene $C_{76}$.[13]
M, multiplicity of corresponding electronic configuration.

**Table 2.** Comparison of relative energies $\Delta E$ (kcal mol$^{-1}$) and HOMO-LUMO gaps (eV) of non-IPR isomer 17418 ($C_1$) and IPR isomer 19150 ($D_2$) of fullerene $C_{76}$ in their neutral and anionic forms (6-31 + G*).

| | ΔE/(HOMO-LUMO) | | | |
|---|---|---|---|---|
| Fullerene $C_{76}$ isomer no. | $C_{76}$ | $C_{76}^{2-}$ | $C_{76}^{4-}$ | $C_{76}^{6-}$ |
| 19150[a] ($D_2$) | 0.00/1.95 | 0.00/0.87 | 0.00/0.80 | 0.00/1.47 |
| 17418 ($C_1$) | 33.10/1.30 | 3.44/1.23 | −4.64/1.03 | −0.21/1.17 |

[a]Most stable IPR isomer of fullerene $C_{76}$.[13]

**Table 3.** Bond lengths in IPR fullerenes $C_{60}$ ($I_h$) and $C_{70}$ ($D_{5h}$) and in non-IPR isomer 17418 ($C_1$) of fullerene $C_{76}$, Å.

| | Single | | Double | | Delocalized | |
|---|---|---|---|---|---|---|
| Isomer no. | min | max | min | max | min | max |
| $C_{60}$ ($I_h$)[60] | 1.459 | | 1.397 | | – | |
| $C_{70}$ ($D_{5h}$)[61] | 1.454 | 1.477 | 1.390 | 1.399 | 1.424 | 1.439 |
| 17418 ($C_1$) singlet, | 1.432 | 1.489 | 1.362 | 1.424 | 1.386 | 1.458 |
| M = 1 | 1.434 | 1.479 | 1.366 | 1.424 | 1.389 | 1.478 |
| triplet, M = 3 | 1.431 | 1.475 | 1.378 | 1.430 | 1.389 | 1.471 |
| quintet, M = 5 | | | | | | |

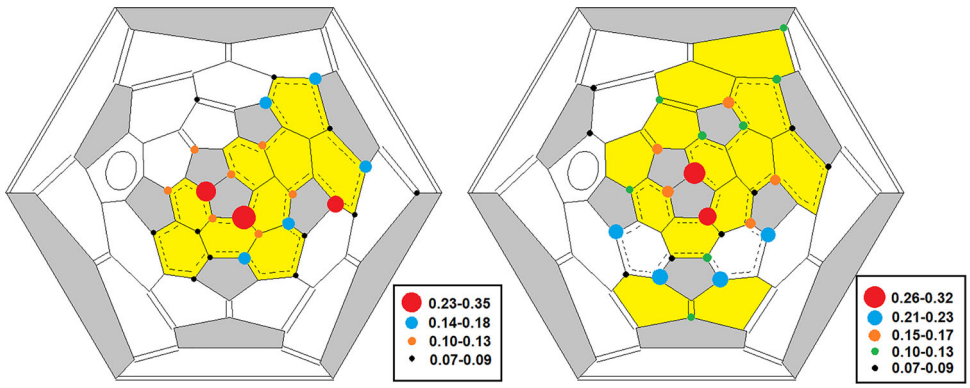


**Figure 3.** The maximum spin densities distribution in triplet (left) and quintet (right) configurations of non-IPR isomer 17418 ($C_1$) of fullerene $C_{76}$; regions with maximum spin densities are depicted by yellow.

metallofullerene U@$C_{76}$ and fully characterized by single crystal X-ray diffractometry. The optimal locations of endohedral atoms slightly disordered over several positions are near the pentalene motif.[40] It should be further noted that the experimentally determined positions of uranium atoms inside the fullerene molecules are close to clusters from pentalene and phenalenyl-radical substructures (Figure 4). It is supporting our argumentation because maximum values of spin densities are located namely here. It means that the addition of extra electrons to the unpaired ones creates a higher electron density, namely at these fragments of molecules, instead of being diffused on the fullerene sphere. Therefore, due to a higher electronic density of these substructures, metal cations shift to them.

One more reason for the stabilization of non-IPR endohedral metallofullerenes should be mentioned. The "folding" of an initially flat pentalene structure (Figure 5) in fullerene molecule leads to significant local overstrains.[6,58,59] The hypothetical molecules of pristine non-IPR isomer 17418 ($C_1$) of fullerene $C_{76}$ show folding angles 46.2–46.6° (Table 4) that means the presence of high overstrains. Its stabilizations in the form of endohedral metallofullerene is explained by strain relaxation ($F = 47.94$) due to the coordination of endohedral atom with pentalene fragments.[62]

Thus, the instability of the studied fullerene is caused by its open-shell structure and by significant local overstrains related to the high folding angle value of pentagons in the pentalene substructure. Taking into account a previous success in the stabilization of non-IPR fullerenes, a key role in the stabilization of such fullerenes can play a decrease in strain, caused, for example, by changing the carbon hybridization from $sp^2$ to $sp^3$ in radical addition reaction or by

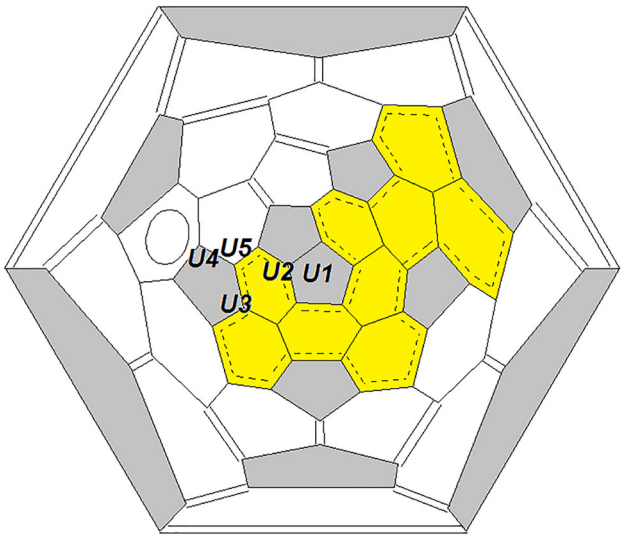


**Figure 4.** The positions of disordered endohedral atoms in U@(17418)-$C_{76}$ together with pentalene and phenalenyl-radical substructures; regions with maximum spin densities are depicted by yellow.

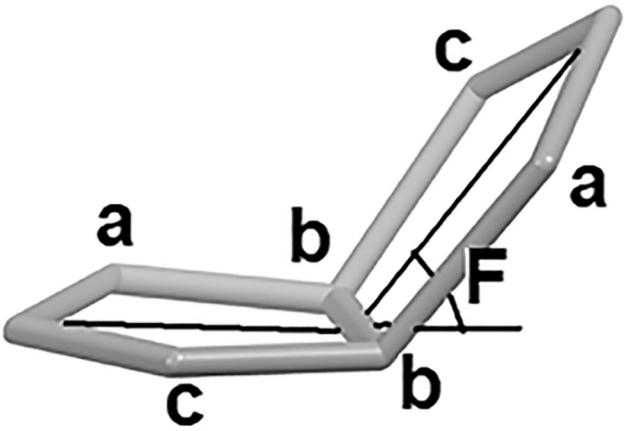


**Figure 5.** Folding angle F of pentalene substructure.

**Table 4.** Dihedral angles and folding angles *F* (grad.) in molecules of isomer 17418 ($C_1$) of pristine fullerene $C_{76}$ and endohedral U@$C_{76}$.

| Fullerene | a-b-b-a[a] | c-b-b-c | aver. | *F* |
|---|---|---|---|---|
| $C_{76}$ 17418 ($C_1$) quintet | 133.17 | 133.62 | 133.39 | 46.61 |
| $C_{76}$ 17418 ($C_1$) triplet | 134.15 | 133.45 | 133.80 | 46.20 |
| U@$C_{76}$, X-ray[40] | 131.78 | 132.34 | 132.06 | 47.94 |

[a]Dihedral angles designations see Figure 5.

coordinating the endohedral metal atom with the substructures consisting from condensed pentagons and/or radical ones in endohedral derivatives. As one of the mechanisms of the synthesis of these non-IPR fullerene endohedral derivatives we suppose the addition of the plasma electrons to the highest spin densities positions of cage precursors, that form a stable ionic pair metal-cage precursor, then finally closing of the fullerene cage.

## 4. Conclusions

Thus, quantum chemical calculations (DFT) show that non-IPR isomer 17418 ($C_1$) of fullerene $C_{76}$ has a radical nature of its electronic structure. The distributions of single, double and delocalized $\pi$-bonds in researched isomer molecules are presented for the first time as well as their molecular formulas. The spin densities are mainly concentrated on atoms of fused pentagons and phenalenyl-radical substructures. Additionally to the radical nature, the main instability reason is the high folding angle between pentagons of substructures with fused pentagons. The previously experimentally determined cations sites inside the fullerene, which stabilize the molecule as a whole, are close to the aforementioned radical clusters.

## Disclosure statement

No potential conflict of interest was reported by the authors.

## Funding

This work was financial support from the government assignment for FRC Kazan Scientific Center of RAS and partially supported by the Russian Foundation for Basic Research under Grant No. 18-29-19110mk.

## ORCID

Ayrat Khamatgalimov http://orcid.org/0000-0002-2865-8619
Denis Chachkov http://orcid.org/0000-0002-0073-3672
Valeri Kovalenko http://orcid.org/0000-0002-9605-3232

## References

[1] Kroto, H. W. The Stability of the Fullerenes $C_n$, with n = 24, 28, 32, 36, 50, 60 and 70. *Nature* **1987**, *329*, 529–531. DOI: 10.1038/329529a0.
[2] Schmalz, T. G.; Seitz, W. A.; Klein, D. J.; Hite, G. E. Elemental Carbon Cages. *J. Am. Chem. Soc.* **1988**, *110*, 1113–1127. DOI: 10.1021/ja00212a020.
[3] Guan, R.; Chen, M.; Jin, F.; Yang, S. Strain Release of Fused Pentagons in Fullerene Cages by Chemical Functionalization. *Angew. Chem. Int. Ed. Engl.* **2020**, *59*, 1048–1073. DOI: 10.1002/anie.201901678.
[4] Kovalenko, V. I.; Khamatgalimov, A. R. Regularities in the Molecular Structure of Stable Fullerenes. *Russ. Chem. Rev.* **2006**, *75*, 981–988. DOI: 10.1070/RC2006v075n11ABEH003620.
[5] Khamatgalimov, A. R.; Kovalenko, V. I. Structures of Unstable Isolated-Pentagon-Rule Fullerenes $C_{72}$-$C_{86}$ Molecules. *Russ. Chem. Rev.* **2016**, *85*, 836–853. DOI: 10.1070/RCR4571.
[6] Kovalenko, V. I.; Khamatgalimov, A. R. *Structure and Stability of Higher Fullerenes*; Publications of the Russian Academy of Science: Moscow, **2019** (in Russian).
[7] Shen, W.; Bao, L.; Yu, S.; Yang, L.; Jin, P.; Xie, Y.; Akasaka, T.; Lu, X. Crystallographic Characterization of $Lu_2C_{2n}$ (*2n* = 76-90): Cluster Selection by Cage Size. *Chem. Sci.* **2019**, *10*, 829–836. DOI: 10.1039/c8sc03886d.
[8] Cai, W.; Alvarado, J.; Metta-Magaña, A.; Chen, N.; Echegoyen, L. Interconversions between Uranium Mono-Metallofullerenes: Mechanistic Implications and Role of Asymmetric Cages. *J. Am. Chem. Soc.* **2020**, *142*, 13112–13119. DOI: 10.1021/jacs.0c04888.
[9] Shustova, N. B.; Kuvychko, I. V.; Bolskar, R. D.; Seppelt, K.; Strauss, S. H.; Popov, A. A.; Boltalina, O. V. Trifluoromethyl Derivatives of Insoluble small-HOMO-LUMO-Gap Hollow Higher Fullerenes. NMR and DFT Structure Elucidation of $C_2$-($C_{74}$-$D_{3h}$)$(CF_3)_{12}$, $C_s$-($C_{76}$-$T_d$(2))$(CF_3)_{12}$, $C_2$-($C_{78}$-$D_{3h}$(5))$(CF_3)_{12}$, $C_s$-($C_{80}$-$C_{2v}$(5))$(CF_3)_{12}$, and $C_2$-($C_{82}$-$C_2$(5))$(CF_3)_{12}$. *J.*

*Am. Chem. Soc.* **2006**, *128*, 15793–15798. DOI: 10.1021/ja065178l.

[10] Fowler, P. W.; Manolopoulos, D. E. *An Atlas of Fullerenes*; Dover Publications: Mineola, New York, **2006**.

[11] Ettl, R.; Chao, I.; Diederich, F.; Whetten, R. L. Isolation of $C_{76}$, a Chiral ($D_2$) Allotrope of Carbon. *Nature* **1991**, *353*, 149–153. DOI: 10.1038/353149a0.

[12] Michel, R. H.; Kappes, M. M.; Adelmann, A.; Roth, G. Preparation and Structure of $C_{76}(S_8)_6$: A First Step in the Crystallographic Investigation of Higher Fullerenes. *Angew. Chem. Int. Ed. Engl.* **1994**, *33*, 1651–1654. DOI: 10.1002/anie.199416511.

[13] Khamatgalimov, A. R.; Kovalenko, V. I. Stability of Isolated-Pentagon-Rule Isomers of Fullerene $C_{76}$. *Fuller. Nanotub. Car. Nanostruct.* **2015**, *23*, 148–152. DOI: 10.1080/1536383X.2012.758114.

[14] Khamatgalimov, A. R.; Kovalenko, V. I. Radical IPR Fullerenes $C_{74}$ ($D_{3h}$) and $C_{76}$ ($T_d$): Dimer, Trimer, Etc. Experiments and Theory. *J. Phys. Chem. C* **2018**, *122*, 3146–3151. DOI: 10.1021/acs.jpcc.7b11940.

[15] Ori, O.; D'Mello, M. A Topological Study of the Structure of the $C_{76}$ Fullerene. *Chem. Phys. Lett* **1992**, *197*, 49–54. DOI: 10.1016/0009-2614(92)86020-I.

[16] Colt, J. R.; Scuseria, G. E. An Ab Initio Study of the $C_{76}$ Fullerene Isomers. *J. Phys. Chem.* **1992**, *96*, 10265–10268. DOI: 10.1021/j100204a032.

[17] Orlandi, G.; Zerbetto, F.; Fowler, P. W.; Manolopoulos, D. E. The Electronic Structure and Vibrational Frequencies of the Stable $C_{76}$ Isomer of $D_2$ Symmetry. *Chem. Phys. Lett.* **1993**, *208*, 441–445. DOI: 10.1016/0009-2614(93)87170-8.

[18] Austin, S. J.; Fowler, P. W.; Orlandi, G.; Manolopoulos, D. E.; Zerbetto, F. Relative Stabilities of $C_{76}$ Isomers. A Numerical Test of the Fullerene Isolated-Pentagon Rule. *Chem. Phys. Lett.* **1994**, *226*, 219–225. DOI: 10.1016/0009-2614(94)00702-0.

[19] Sun, G.; Kertesz, M. Theoretical $^{13}C$ NMR Spectra of IPR Isomers of Fullerenes $C_{60}$, $C_{70}$, $C_{72}$, $C_{74}$, $C_{76}$, and $C_{78}$ Studied by Density Functional Theory. *J. Phys. Chem. A* **2000**, *104*, 7398–7403. DOI: 10.1021/jp001272r.

[20] Zheng, G.; Irle, S.; Morokuma, K. Performance of the DFTB Method in Comparison to DFT and Semiempirical Methods for Geometries and Energies of $C_{20}$–$C_{86}$ Fullerene Isomers. *Chem. Phys. Lett.* **2005**, *412*, 210–216. DOI: 10.1016/j.cplett.2005.06.105.

[21] Epple, L.; Amsharov, K. Y.; Jansen, M. Structures of the Individual Higher Fullerene Isomers $C_{76}$-$D_2$ and $C_{78}(2)$-$C_{2v}$ in Cocrystals with Ag- and Cu- Tetraphenylporphyrines. *Fuller. Nanotub. Car. Nanostruct.* **2009**, *17*, 67–77. DOI: 10.1080/15363830802519420.

[22] Xu, J.; Lu, X.; Zhou, X.; He, X.; Shi, Z.; Gu, Z. Synthesis, Isolation, and Spectroscopic Characterization of Ytterbium-Containing Metallofullerenes. *Chem. Mater.* **2004**, *16*, 2959–2964. DOI: 10.1021/cm049639i.

[23] Okazaki, T.; Lian, Y.; Gu, Z.; Suenaga, K.; Shinohara, H. Isolation and Spectroscopic Characterization of Sm-Containing Metallofullerenes. *Chem. Phys. Lett.* **2000**, *320*, 435–440.

[24] Tamm, N. B.; Sidorov, L. N.; Troyanov, S. I. Investigations in the Field of Higher Fullerenes. *Moscow Univ. Chem. Bull.* **2009**, *64*, 327–342. DOI: 10.3103/S0027131409060017.

[25] Kareev, I. E.; Popov, A. A.; Kuvychko, I. V.; Shustova, N. B.; Lebedkin, S. F.; Bubnov, V. P.; Anderson, O. P.; Seppelt, K.; Strauss, S. H.; Boltalina, O. V. Synthesis and X-Ray or NMR/DFT Structure Elucidation of Twenty-One New Trifluoromethyl Derivatives of Soluble Cage Isomers of $C_{76}$, $C_{78}$, $C_{84}$, and $C_{90}$. *J. Am. Chem. Soc.* **2008**, *130*, 13471–13489. DOI: 10.1021/ja8041614.

[26] Tamm, N. B.; Troyanov, S. I. Trifluoromethyl Derivatives of Fullerene $C_{76}$, $C_{76}(CF_3)_{14-18}$. *Mendeleev Commun.* **2010**, *20*, 229–230. DOI: 10.1016/j.mencom.2010.06.016.

[27] Lanskikh, M. A.; Belova, Y. M.; Tamm, N. B.; Chang, K.; Kemnitz, E.; Troyanov, S. I. Crystal and Molecular Structures of Trifluoromethyl Derivatives of Fullerenes $C_{76}$ and $C_{82}$. *Crystallogr. Rep.* **2011**, *56*, 1047–1053. DOI: 10.1134/S1063774511050178.

[28] Umemoto, H.; Ohashi, K.; Inoue, T.; Fukui, N.; Sugai, T.; Shinohara, H. Synthesis and UHV-STM Observation of the Td-Symmetric Lu Metallofullerene: $Lu_2@C_{76}(T_d)$. *Chem. Commun.* **2010**, *46*, 5653–5655. DOI: 10.1039/c0cc00824a.

[29] Yang, S.; Popov, A. A.; Dunsch, L. The Role of an Asymmetric Nitride Cluster on a Fullerene Cage: The non-IPR Endohedral $DySc_2N@C_{76}$. *J. Phys. Chem. B* **2007**, *111*, 13659–13663. DOI: 10.1021/jp709650d.

[30] Suzuki, M.; Mizorogi, N.; Yang, T.; Uhlik, F.; Slanina, Z.; Zhao, X.; Yamada, M.; Maeda, Y.; Hasegawa, T.; Nagase, S.; et al. $La_2@C_s(17\,490)$-$C_{76}$: A New Non-IPR Dimetallic Metallofullerene Featuring Unexpectedly Weak Metal–Pentalene Interactions. *Chem. Eur. J.* **2013**, *19*, 17125–17130. DOI: 10.1002/chem.201302821.

[31] Slanina, Z.; Uhlík, F.; Lee, S.-L.; Wang, B.-C.; Adamowicz, L.; Suzuki, M.; Haranaka, M.; Feng, L.; Lu, X.; Nagase, S.; et al. Towards Relative Populations of Non-Isomeric Metallofullerenes: $La@C_{76}(T_d)$ vs. $La_2@C_{76}(C_s,17490)$. *Fuller. Nanotub. Car. Nanostruct.* **2014**, *22*, 299–306. DOI: 10.1080/1536383X.2013.863764.

[32] Yang, T.; Zhao, X.; Xu, Q.; Zhou, C.; He, L.; Nagase, S. Non-IPR Endohedral Fullerene $Yb@C_{76}$: density Functional Theory Characterization. *J. Mater. Chem.* **2011**, *21*, 12206–12209. DOI: 10.1039/c1jm12230d.

[33] Hao, Y.; Feng, L.; Xu, W.; Gu, Z.; Hu, Z.; Shi, Z.; Slanina, Z.; Uhlík, F. $Sm@C_{2v}(19138)$-$C_{76}$: A Non-IPR Cage Stabilized by a Divalent Metal Ion. *Inorg. Chem.* **2015**, *54*, 4243–4248. DOI: 10.1021/ic502911v.

[34] Liu, F.; Wang, S.; Gao, C.-L.; Deng, Q.; Zhu, X.; Kostanyan, A.; Westerström, R.; Jin, F.; Xie, S.-Y.; Popov, A. A.; et al. Mononuclear Clusterfullerene Single-Molecule Magnet Containing Strained Fused-Pentagons Stabilized by a Nearly Linear Metal Cyanide Cluster. *Angew. Chem. Int. Ed. Engl.* **2017**, *56*, 1830–1834. DOI: 10.1002/anie.201611345.

[35] Slanina, Z.; Uhlík, F.; Feng, L.; Adamowicz, L. Evaluation of the Relative Stabilities of Two non-IPR Isomers of $Sm@C_{76}$. *Fuller. Nanotub. Car. Nanostruct.* **2016**, *24*, 339–344. DOI: 10.1080/1536383X.2016.1139576.

[36] Yang, T.; Zhao, X.; Xu, Q.; Zheng, H.; Wang, W. W.; Li, S. T. Probing the Role of Encapsulated Alkaline Earth Metal Atoms in Endohedral Metallofullerenes $M@C_{76}$ (M = Ca, Sr, and Ba) by First-Principles Calculations. *Dalton Trans.* **2012**, *41*, 5294–5300. DOI: 10.1039/c2dt12420c.

[37] Meng, Q.-Y.; Wang, D.-L.; Xin, G.; Li, T.-C.; Hou, D.-Y. Linear Monometallic Cyanide Cluster Fullerenes $ScCN@C_{76}$ and $YCN@C_{76}$: A Theoretical Prediction. *Comp. Theor. Chem.* **2014**, *1050*, 83–88. DOI: 10.1016/j.comptc.2014.10.019.

[38] Gao, F.-W.; Xu, H.-L.; Su, Z.-M. The Inner-Induced Effects of YCN in $C_{76}$ on the Structures and Nonlinear Optical Properties. *J. Mol. Model.* **2016**, *22*, 1–7. 174 (

[39] Zhao, P.; Yang, T.; Guo, Y.-J.; Dang, J.-S.; Zhao, X.; Nagase, S. Dimetallic Sulfide Endohedral Metallofullerene $Sc_2S@C_{76}$: Density Functional Theory Characterization. *J. Comput. Chem.* **2014**, *35*, 1657–1663. DOI: 10.1002/jcc.23671.

[40] Cai, W.; Abella, L.; Zhuang, J.; Zhang, X.; Feng, L.; Wang, Y.; Morales-Martínez, R.; Esper, R.; Boero, M.; Metta, M.; et al. Synthesis and Characterization of non-Isolated-Pentagon-Rule Actinide Endohedral Metallofullerenes $U@C_1(17418)$-$C_{76}$, $U@C_1(28324)$-$C_{80}$, and $Th@C_1(28324)$-$C_{80}$: Low-Symmetry Cage Selection Directed by a Tetravalent Ion. *J. Am. Chem. Soc.* **2018**, *140*, 18039–18050. DOI: 10.1021/jacs.8b10435.

[41] Zhao, P.; Zhao, X.; Ehara, M. Theoretical Insights into Monometallofullerene $Th@C_{76}$: Strong Covalent Interaction between Thorium and the Carbon Cage. *Inorg. Chem.* **2018**, *57*, 2961–2964. DOI: 10.1021/acs.inorgchem.7b03114.

[42] Ioffe, I. N.; Goryunkov, A. A.; Tamm, N. B.; Sidorov, L. N.; Kemnitz, E.; Troyanov, S. I. Fusing Pentagons in a Fullerene

Cage by Chlorination: IPR $D_2$-$C_{76}$ Rearranges into non-IPR $C_{76}Cl_{24}$. *Angew. Chem. Int. Ed.* **2009**, *48*, 5904–5907. DOI: 10.1002/anie.200902253.

[43] Ioffe, I. N.; Mazaleva, O. N.; Chen, C.; Yang, S.; Kemnitz, E.; Troyanov, S. I. $C_{76}$ Fullerene Chlorides and Cage Transformations. Structural and Theoretical Study. *Dalton Trans.* **2011**, *40*, 11005–11011. DOI: 10.1039/c1dt10256g.

[44] Sudarkova, S. M.; Mazaleva, O. N.; Konoplev-Esgenburg, R. A.; Troyanov, S. I.; Ioffe, I. N. Versatility of Chlorination-Promoted Skeletal Transformation Pathways in $C_{76}$ Fullerene. *Dalton Trans.* **2018**, *47*, 4554–4559. DOI: 10.1039/c8dt00245b.

[45] Yang, S.; Ioffe, I. N.; Troyanov, S. I. Chlorination-Promoted Skeletal Transformations of Fullerenes. *Acc. Chem. Res.* **2019**, *52*, 1783–1792. DOI: 10.1021/acs.accounts.9b00175.

[46] Tamm, N. B.; Brotsman, V. A.; Markov, V. Y.; Kemnitz, E.; Troyanov, S. I. Chlorination-Promoted Skeletal Transformation of IPR $C_{76}$ Discovered via Trifluoromethylation under the Formation of non-IPR $C_{76}(CF_3)_nF_m$. *Dalton Trans.* **2018**, *47*, 6898–6902. DOI: 10.1039/C8DT00984H.

[47] Khamatgalimov, A. R.; Idrisov, R. I.; Kamaletdinov, I. I.; Kovalenko, V. I. The Key Feature of Instability of Small non-IPR Closed-Shell Fullerenes: three Isomers of $C_{40}$. *Mendeleev. Commun.* **2020**, *30*, 725–727. DOI: 10.1016/j.mencom.2020.11.012.

[48] Khamatgalimov, A. R.; Idrisov, R. I.; Kamaletdinov, I. I.; Kovalenko, V. I. Open-Shell Nature of non-IPR Fullerene $C_{40}$: isomers 29 (*C2*) and 40 (*Td*). *J. Mol. Model.* **2021**, *27*, 22.

[49] Khamatgalimov, A. R.; Yakupova, L. I.; Kovalenko, V. I. Features of Molecular Structure of Small non-IPR Fullerenes: The Two Isomers of $C_{50}$. *Theor. Chem. Acc.* **2020**, *139*, 159.

[50] Frisch, M. J.; Trucks, G. W.; Schlegel, H. B.; Scuseria, G. E.; Robb, M. A.; Cheeseman, J. R.; Scalmani, G.; Barone, V.; Mennucci, B.; Petersson, G. A.; et al. *Gaussian 09*, Revision A.1; Gaussian, Inc.: Wallingford, CT, **2009**.

[51] Becke, A. D. Density-Functional Thermochemistry. III. The Role of Exact Exchange. *J. Chem. Phys.* **1993**, *98*, 5648–5652. DOI: 10.1063/1.464913.

[52] Lee, C.; Yang, W.; Parr, R. G. Development of the Colle-Salvetti Correlation-Energy Formula into a Functional of the Electron Density. *Phys. Rev. B Condens. Matter*. **1988**, *37*, 785–789. DOI: 10.1103/physrevb.37.785.

[53] Khamatgalimov, A. R.; Kovalenko, V. I. Electronic Structure and Stability of Fullerene $C_{82}$ Isolated-Pentagon-Rule Isomers. *J. Phys. Chem. A* **2011**, *115*, 12315–12320. DOI: 10.1021/jp204565q.

[54] Olmstead, M. M.; Bettencourt-Dias, A.; Stevenson, S.; Dorn, H. C.; Balch, A. L. Crystallographic Characterization of the Structure of the Endohedral Fullerene [$Er_2$@$C_{82}$ isomer I] with C cage Symmetry and Multiple Sites for Erbium Along a Band of Ten Contiguous Hexagons. *J. Am. Chem. Soc.* **2002**, *124*, 4172–4173. DOI: 10.1021/ja0116019.

[55] Mercado, B. Q.; Chen, N.; Rodríguez-Fortea, A.; Mackey, M. A.; Stevenson, S.; Echegoyen, L.; Poblet, J. M.; Olmstead, M. M.;; Balch, A. L. The Shape of the $Sc_2(\mu_2\text{-S})$ Unit Trapped in $C_{82}$: crystallographic, Computational, and Electrochemical Studies of the Isomers, $Sc_2(\mu_2\text{-S})$@*Cs*(6)-$C_{82}$ and $Sc_2(\mu_2\text{-S})$@$C_3v$(8)-$C_{82}$. *J. Am. Chem. Soc.* **2011**, *133*, 6752–6760. DOI: 10.1021/ja200289w.

[56] Yang, H.; Jin, H.; Wang, X.; Liu, Z.; Yu, M.; Zhao, F.; Mercado, B. Q.; Olmstead, M. M.; Balch, A. A. X-Ray Crystallographic Characterization of New Soluble Endohedral Fullerenes Utilizing the Popular $C_{82}$ Bucky Cage. Isolation and Structural Characterization of Sm@$C_{3v}$(7)-$C_{82}$, Sm@C(6)-$C_{82}$, and Sm@$C_2$(5)-$C_{82}$. *J. Am. Chem. Soc.* **2012**, *134*, 14127–14136. DOI: 10.1021/ja304867j.

[57] Konishi, A.; Okada, Y.; Nakano, M.; Sugisaki, K.; Sato, K.; Takui, T.; Yasuda, M. Synthesis and Characterization of Dibenzo[*a,f*]Pentalene: harmonization of the Antiaromatic and Singlet Biradical Character. *J. Am. Chem. Soc.* **2017**, *139*, 15284–15287. DOI: 10.1021/jacs.7b05709.

[58] Tan, Y.-Z.; Xie, S.-Y.; Huang, R.-B.; Zheng, L.-S. The Stabilization of Fused-Pentagon Fullerene Molecules. *Nat. Chem.* **2009**, *1*, 450–460. DOI: 10.1038/nchem.329.

[59] Deng, Q.; Popov, A. A. Clusters Encapsulated in Endohedral Metallofullerenes: How Strained Are They? *J. Am. Chem. Soc.* **2014**, *136*, 4257–4264. DOI: 10.1021/ja4122582.

[60] Hedberg, K.; Hedberg, L.; Bethune, D. S.; Brown, C. A.; Dorn, H. C.; Johnson, R. D.; de Vries, M. Bond Lengths in Free Molecules of Buckminsterfullerene, $C_{60}$, from Gas-Phase Electron Diffraction. *Science* **1991**, *254*, 410–412. DOI: 10.1126/science.254.5030.410.

[61] Hedberg, K.; Hedberg, L.; Buhl, M.; Bethune, D. S.; Brown, C. A.; Johnson, R. D. Molecular Structure of Free Molecules of the Fullerene $C_{70}$ from Gas-Phase Electron Diffraction. *J. Am. Chem. Soc.* **1997**, *119*, 5314–5320. DOI: 10.1021/ja970110e.

[62] Summerscales, O. T.; Cloke, F. G. N. The Organometallic Chemistry of Pentalene. *Coord. Chem. Rev.* **2006**, *250*, 1122–1140. DOI: 10.1016/j.ccr.2005.11.020.